Journal of Theoretical Biology 462 (2019) 408–417

Contents lists available at ScienceDirect

Journal of Theoretical Biology

journal homepage: www.elsevier.com/locate/jtb

A metapopulation model of dog rabies transmission in N'Djamena, Chad

Mirjam Laager[a,b,*], Monique Léchenne[a,b], Kemdongarti Naissengar[c], Rolande Mindekem[d], Assandi Oussiguere[c], Jakob Zinsstag[a,b], Nakul Chitnis[a,b]

[a] Swiss Tropical and Public Health Institue, Socinstrasse 57, Basel 4051, Switzerland
[b] University of Basel, Petersplatz 1, Basel 4001, Switzerland
[c] Institut de Recherches en Elevage pour le Développement, BP 433, Farcha, N'Djamena, Chad
[d] Centre de Support en Santé Internationale, BP 972, Moursal, N'Djamena, Chad

ARTICLE INFO

Article history:
Received 5 July 2017
Revised 22 November 2018
Accepted 26 November 2018
Available online 27 November 2018

Keywords:
Epidemiological model
Rabies control

ABSTRACT

Rabies transmission was interrupted for several months in N'Djamena, the capital city of Chad, after two mass vaccination campaigns of dogs. However, there was a resurgence in cases, which was not predicted by previous models of rabies transmission. We developed a deterministic metapopulation model with importation of latent dogs, calibrated to four years of weekly incidence data from passive surveillance, to investigate possible causes for the early resurgence. Our results indicate that importation of latently infective dogs better explains the data than heterogeneity or underreporting. Stochastic implementations of the model suggest that the two vaccination campaigns averted approximately 67 cases of dog rabies (out of an estimated 74 cases without vaccination) and 124 human exposures (out of an estimated 148 human exposures without vaccination) over two years. Dog rabies vaccination is therefore an effective way of preventing rabies in the dog population and to subsequently reduce human exposure. However, vaccination campaigns have to be repeated to maintain the effect or reintroduction through importation has to be prevented.

1. Introduction

Rabies is a viral disease that is transmitted by bite and can affect any mammal. After the onset of symptoms, rabies is fatal. Approximately 59,000 people die of rabies every year (Hampson et al., 2015), mainly in developing countries with children most at risk. The main vector for human rabies is the domestic dog. Rabies in humans can be prevented by vaccinating dogs or by post exposure treatment of humans, which consists of vaccination and injection of immunoglobulin (World Health Organization, 2010). Pre-exposure vaccination is also available, which simplifies the post exposure regimen and has been recommended in places with high dog bite incidence, incomplete rabies control in the animal reservoir and limited access to immunoglobulin (Kessels et al., 2017; World Health Organization, 2013).

Detailed analysis of rabies transmission biology suggests that rabies has a low reproductive ratio (Hampson et al., 2009) and that with a sufficiently high dog rabies vaccination coverage, rabies could be eliminated (Fahrion et al., 2017; Fooks et al., 2014; Lankester et al., 2014; Lembo et al., 2010). Dog rabies vaccination can be an effective path of preventing human exposure, avoiding the very expensive post exposure treatment. However maintaining vaccination coverage over a longer time is crucial, as has been seen in the recent case of rabies reintroduction in Arequipa (Castillo-Neyra et al., 2017).

Mathematical models offer a framework to compare the effect of different interventions on disease transmission dynamics, with a long history of application to rabies. Anderson et al. (1981) developed a deterministic ordinary differential equation model to simulate the dynamics of rabies transmission among foxes in Europe, assuming density dependent transmission and logistic population dynamics of foxes. They concluded that culling is unlikely to be an effective intervention and recommended compulsory vaccination of cats and dogs. Murray et al. (1986) modified the model by Anderson et al. by adding a diffusion term to incorporate spatial

* Corresponding author at: Epidemiology and Public Health, Socinstrasse 57, Basel, Switzerland.
E-mail address: mirjam.laager@unibas.ch (M. Laager).

https://doi.org/10.1016/j.jtbi.2018.11.027

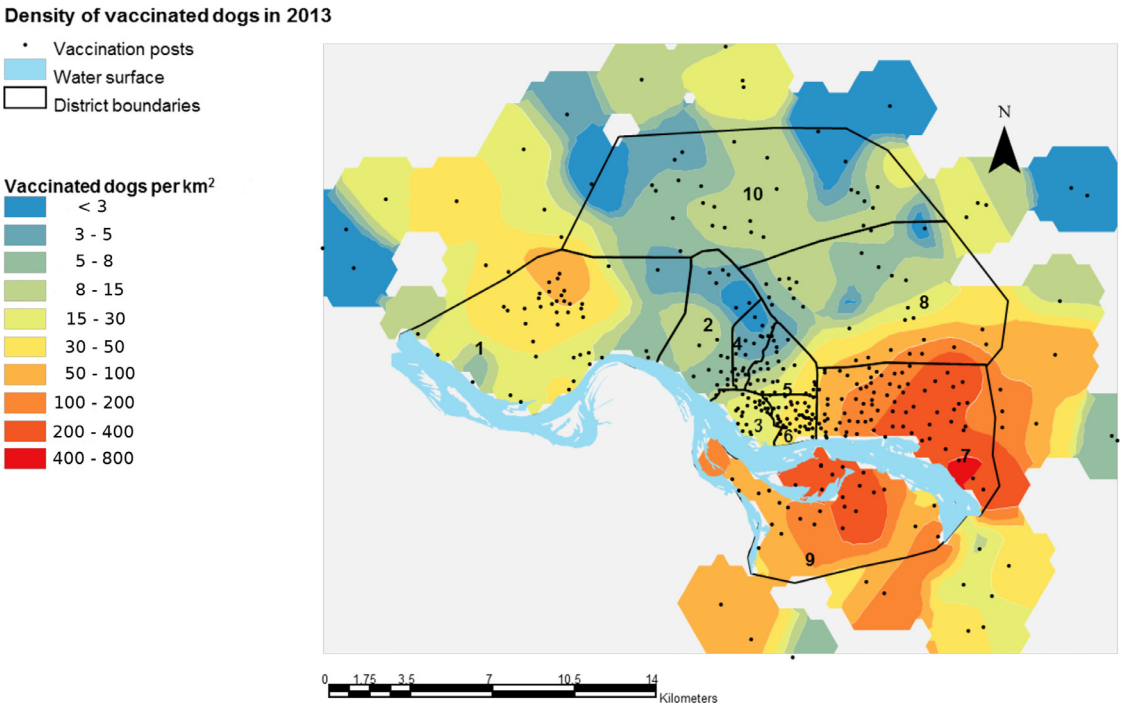

Fig. 1. Districts of N'Djamena and density of vaccinated dogs in 2013 (Figure reproduced from Zinsstag et al. (2017)).

dispersal of rabid foxes. They determined the minimal speed of the travelling wavefront for different diffusion coefficients and applied these results to a hypothetical fox rabies outbreak in the south of England. Ou and Wu (2006) introduced a distinct movement behaviour of adult and juvenile foxes, which yields a system of reaction diffusion equations with delayed nonlinear interactions. Using finite elements for space discretization of a system of partial differential equations, Keller et al. (2013) simulated the spread of raccoon rabies on a fine grid incorporating landscape heterogeneities such as rivers, forests and highways.

While models for rabies in wildlife populations such as foxes and raccoons often use random diffusion to incorporate space in the model and are interested in movement over large areas, models of transmission in dogs have to take into account that movement of domestic dogs is likely to be centred around the residences of the owners. Several models of dog rabies transmission have addressed this. Dürr et al. collected detailed geopositioning system (GPS) data on dog movement in Australia (Dürr and Ward, 2014) and developed an individual based, stochastic transmission model where the transmission probability between two dogs decreased with distance between the owners households according to a function that was estimated from the movement behaviour data (Dürr and Ward, 2015). Beyer et al. (2011) fitted a stochastic metapopulation model of 75 villages in Tanzania to incidence data, assuming that transmission probability decreases exponentially with distance between households. Chen et al. (2015) modelled the spread of rabies in Mainland China by using a deterministic compartmental model in each province and assuming movement of dogs between the provinces.

In N'Djamena, the capital of Chad, two mass vaccination campaigns of dogs were conducted in 2012 and 2013, reaching a vaccination coverage of 70% in both years, as described in more detail in a previous publication (Léchenne et al., 2016). During a period of 13 weeks, from October to January, vaccination posts were set up in all districts of N'Djamena (Fig. 1). Dogs were brought to the vaccination posts by the owners and were vaccinated free of charge. After the vaccination, a certificate was issued and the vaccinated dogs were marked with a collar. The weekly number of vaccinated dogs ranged from 24 to 4402 dogs and the total number of vaccinated dogs after 13 weeks was 17,538 in 2012 and 21,340 in 2013. Coverage was assessed with a capture-mark-recapture model. Since 2012, weekly incidence of rabies in dogs was reported through passive surveillance. Before the campaigns, there was on average one confirmed case of dog rabies per week. The campaigns interrupted transmission for 8 months, but there was a resurgence in cases, which was not predicted by a previous model of rabies transmission (Zinsstag et al., 2017). Possible reasons for the early resurgence include heterogeneity, reintroduction and underreporting. Dog densities and vaccination coverage varied largely across the different districts of N'Djamena (Fig. 1) and this heterogeneity could facilitate early re-establishment of rabies in the population in higher transmission districts. A previous study in Bangui showed that reintroduction of strains from outside the city occurs frequently (Bourhy et al., 2016), which could also explain the early resurgence seen in N'Djamena. Rabies cases are also frequently underreported (Hampson et al., 2015). Each case in the passive surveillance data was confirmed by an immunofluorescence antibody test (IFAT) which implies that all recorded cases are true cases. However, since passive surveillance is based on voluntary reporting, there could be many additional cases. The resurgence seen in the data could therefore also be explained by unreported ongoing transmission.

We develop a deterministic ordinary differential equation model to explore which one of these reasons best explains the resurgence. We incorporate heterogeneity by dividing the city into patches, with a homogeneous model in each patch and some movement of infections between patches and allow for the importation of latent dogs from the surroundings of the city. We fit the model parameters to the four years of weekly incidence data and conduct a sensitivity analysis to assess the effect of underreporting on the estimated transmission rates. A stochastic version of the model, implemented via the Gillespie algorithm, yields a distribution of the time to elimination.

Table 1
State variables of the transmission models. For the homogeneous model, state variables have no subscript k.

Variable	Description
$S_k(t)$	Number of susceptible dogs in patch k at time t
$E_k(t)$	Number of exposed dogs in patch k at time t
$I_k(t)$	Number of rabid dogs in patch k at time t
$V_k(t)$	Number of vaccinated dogs in patch k at time t

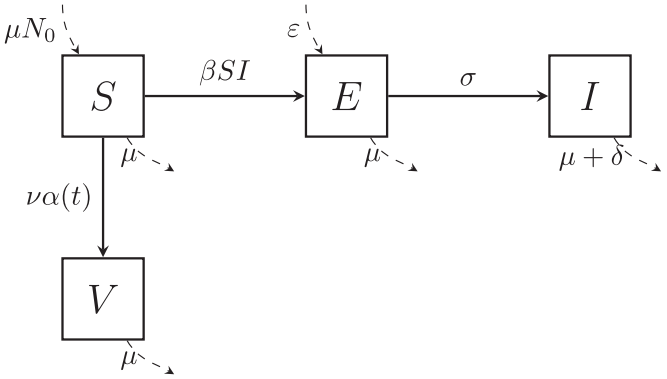

Fig. 2. Schematic of the homogeneous model.

2. Model description

2.0.0.1. Homogeneous model. We use a deterministic ordinary differential equation model, based on a previous model (Zinsstag et al., 2009, 2017), where the population is divided into susceptible (S), exposed (E), infective (I) and vaccinated (V) dogs. As in the previous model and in many deterministic models of rabies transmission (Anderson et al., 1981; Chen et al., 2015; Murray et al., 1986; Ou and Wu, 2006), dogs become exposed via density dependent transmission and die from rabies according to a per capita disease induced death rate. The previous model assumed logistic population dynamics of dogs with a quadratic death rate. We simplified the model by assuming a constant birth and a constant per-capita death rate. We also removed the vaccination of exposed dogs, since we found no evidence that dogs can still be successfully protected after an infectious bite. A study showed that 88% of dogs vaccinated with a single dose against rabies still survived a challenge with live rabies virus after three years (Lakshmanan et al., 2006), so we assume that vaccinated dogs stay protected for the rest of their lives. We also allowed for the importation of latent dogs into the population.

The equations for the homogeneous model are given by

$$\frac{dS(t)}{dt} = \mu N_0 - (\nu\alpha(t) + \mu)S(t) - \beta S(t)I(t), \tag{1a}$$

$$\frac{dE(t)}{dt} = \beta S(t)I(t) - (\sigma + \mu)E(t) + \varepsilon, \tag{1b}$$

$$\frac{dI(t)}{dt} = \sigma E(t) - (\delta + \mu)I(t), \tag{1c}$$

$$\frac{dV(t)}{dt} = \nu\alpha(t)S(t) - \mu V(t). \tag{1d}$$

The description of the state variables and parameters can be found in the Tables 1 and 2 (ignoring the indices of the patches). A schematic of the model is shown in Fig. 2. All rates are constant in time, except for the vaccination rate, which is given by

$$\alpha(t) = \alpha^* + \alpha_0^{(i)}(t) + \alpha_1^{(i)}(t)e^{-\varphi_\alpha t}, \tag{2}$$

where α^* is a background vaccination rate and $\alpha_0^{(i)}$ and $\alpha_1^{(i)}$ are fitted to the number of vaccinated dogs in each week i of the vaccination campaigns in N'Djamena, and φ_α is a saturation parameter, as explained in more detail in the section on model calibration.

Metapopulation model. We expand the homogeneous model described above to a metapopulation model with n subpopulations. In each subpopulation the population dynamics are described by

$$\frac{dS_k(t)}{dt} = \mu N_{0,k} - (\nu\alpha_k(t) + \mu)S_k(t) - \beta_k S_k(t)\sum_{j=1}^{n} m_{kj}I_j(t), \tag{3a}$$

$$\frac{dE_k(t)}{dt} = \beta_k S_k(t)\sum_{j=1}^{n} m_{kj}I_j(t) - (\sigma + \mu)E_k(t) + \varepsilon_k, \tag{3b}$$

$$\frac{dI_k(t)}{dt} = \sigma E_k(t) - (\delta + \mu)I_k(t), \tag{3c}$$

$$\frac{dV_k(t)}{dt} = \nu\alpha_k(t)S_k(t) - \mu V_k(t), \tag{3d}$$

where $\alpha_k(t)$, is given by

$$\alpha_k(t) = \alpha_k^* + \alpha_{0,k}^{(i)}(t) + \alpha_{1,k}^{(i)}(t)e^{-\varphi_\alpha t}. \tag{4}$$

The state variables and the parameters are described in Tables 1 and 2.

Since we consider a population of owned dogs we assume Lagrangian movement, which means that there is no exchange of dogs between the patches, but only movement of infection (unlike the model in Chen et al. (2015)). All dogs live in their home patch, but infected dogs can infect susceptible dogs in adjacent patches. These between patch dynamics are captured by the matrix $M = (m_{kj})_{k,j=1}^{n}$, where m_{kj} describes the proportion of time an infected dog from patch j spends in patch k. We impose the following three conditions on M:

(C I) $m_{kj} = m_{kj}$ for all k, j,
(C II) $m_{kk} \geq m_{kj}$ for all j,
(C III) $\sum_{j=1}^{n} m_{kj} = 1$ for all k.

The first and second condition imply that a dog from patch k spends as much time in patch j as any dog from patch j spends in patch k and that a dog spends most time in the patch where its owner lives. The third condition is a normalization that assures, that the sum of the proportional time spent in all patches is one. In the case of no movement this model simplifies to n homogeneous models like the ones described by Eqs. (1).

Stochastic implementation of the model. We use the Gillespie algorithm (Gillespie, 1977) to simulate the time evolution of the stochastic counterpart of the model described by Eqs. (1). For transition rates dependent on the parameter values and state variables at any point in time the algorithm randomly draws a time step based on the sum of all the transition rates and then selects one of all the possible events according to their relative probabilities. Implementing the transitions between the states of the model as a stochastic process allows us to account for unlikely events, to model the importation of exposed dogs as discrete importation events at random points in time and to gain insight into the distribution of the time to elimination.

3. Model analysis

3.1. Homogeneous model without importation

Table 2
Parameters of the transmission models. Time is measured in weeks. For the homogeneous model, the parameters $N_{0,k}$, β_k, $\alpha_k(t)$ and ε_k have no subscript k.

	Description	Dimension	Conditions
μ	Birth/death rate	1/time	$\mu > 0$
$N_{0,k}$	Stable dog population in patch k in the absence of disease	animals	$N_0 > 0$
β_k	Transmission rate in patch k	1/(animals × time)	$\beta_k > 0$
σ	Rate of progression from exposed to infectious state	1/time	$\sigma > 0$
δ	Disease induced death rate	1/time	$\delta > 0$
$\alpha_k(t)$	Vaccination rate in patch k at time t	1/time	$\alpha_k(t) \geq 0$, $\alpha_k(t) \in \mathcal{C}^0(\mathbb{R})$
ν	Efficacy of vaccine	dimensionless	$0 \leq \nu \leq 1$
ε_k	Rate of importation of exposed dogs into patch k	animals	$\varepsilon_k \geq 0$
m_{kj}	Proportion of time a dog from patch j spends in patch k	dimensionless	$0 \leq m_{kj} \leq 1$

Disease free equilibrium and reproductive number. In the absence of importation ($\varepsilon = 0$) and with a constant vaccination rate $\alpha(t) = \alpha^*$ the disease free equilibrium of the homogeneous model is given by

$$S^* = \frac{\mu}{\mu + \nu\alpha^*} N_0, E^* = I^* = 0 \text{ and } V^* = \frac{\nu\alpha^*}{\mu + \nu\alpha *} N_0. \tag{5}$$

We use the next generation matrix approach described by Diekmann et al. (2010) and define the basic reproductive ratio, R_0, as the number of secondary infections, one infectious individual produces over the course of its infectious period in the absence of interventions (also excluding vaccination ($\alpha^* = 0$)). In the homogeneous model the basic reproductive ratio is given by

$$R_0 = \frac{\beta\sigma N_0}{(\sigma + \mu)(\delta + \mu)},$$

and the disease free equilibrium is

$$S^* = N_0, E^* = I^* = V^* = 0. \tag{6}$$

Theorem 1. *The disease free equilibrium (6) is locally asymptotically stable if $R_0 < 1$ and unstable if $R_0 > 1$.*

Proof. The eigenvalues of the Jacobian of the homogeneous model (1) evaluated at the disease free equilibrium in the absence of vaccination are the roots x of the characteristic equation

$$(\mu + x)\left[x^3 + a_2x^2 + a_1x + a_0\right] = 0 \tag{7}$$

with $a_2 = \sigma + \delta + 3\mu, a_1 = (\sigma + \mu)(\delta + \mu) + (\sigma + \mu)\mu + (\delta + \mu)\mu - \sigma\beta N_0$ and $a_0 = (\sigma + \mu)(\delta + \mu)\mu - \sigma\mu\beta N_0$. From the Routh–Hurwitz criterion we know, that these eigenvalues all have negative real parts if and only if $a_2 > 0$, $a_0 > 0$ and $a_2a_1 > a_0$ which is true if and only if $R_0 < 1$.

□

Endemic equilibrium. The endemic equilibrium is given by

$$S^* = \frac{(\sigma + \mu)(\delta + \mu)}{\sigma\beta}, \tag{8a}$$

$$E^* = \frac{\delta + \mu}{\sigma}\left(\frac{\sigma\mu N_0}{(\sigma + \mu)(\delta + \mu)} - \frac{\nu\alpha^* + \mu}{\beta}\right), \tag{8b}$$

$$I^* = \frac{\sigma\mu N_0}{(\sigma + \mu)(\delta + \mu)} - \frac{\nu\alpha^* + \mu}{\beta}, \tag{8c}$$

$$V^* = \frac{\nu\alpha^*(\sigma + \mu)(\delta + \mu)}{\sigma\beta\mu}. \tag{8d}$$

Theorem 2. *In the absence of vaccination ($\alpha^* = 0$) the endemic equilibrium (8) is locally asymptotically stable if and only if $R_0 > 1$.*

Proof. The eigenvalues of the Jacobian of the homogeneous model (1) evaluated at the endemic equilibrium in the absence of vaccination are the roots x of the characteristic equation

$$(\mu + x)\left[x^3 + a_2x^2 + a_1x + a_0\right] = 0 \tag{9}$$

with $a_2 = 2\mu + \sigma + \delta + \frac{\sigma\beta\mu N_0}{(\sigma+\mu)(\delta+\mu)}, a_1 = (2\mu + \sigma + \delta)\frac{\sigma\beta\mu N_0}{(\sigma+\mu)(\delta+\mu)}$ and $a_0 = \mu(\sigma\beta N_0 - (\sigma + \mu)(\delta + \mu))$. From the Routh–Hurwitz criterion we know, that these eigenvalues all have negative real parts if and only if $a_2 > 0$, $a_0 > 0$ and $a_2a_1 > a_0$ which is true if and only if $R_0 > 1$. □

3.2. Homogeneous model with importation

The homogeneous model with importation has no disease free equilibrium. To calculate the endemic equilibrium, we simplify the system of Eqs. (1) to the quadratic equation

$$aI^2 + bI + c = 0$$

with $a = -\beta(\sigma + \mu)(\delta + \mu)$, $b = \sigma\beta\mu N_0 + \sigma\beta\epsilon - (\alpha + \mu)(\sigma + \mu)(\delta + \mu)$ and $c = \sigma\epsilon(\alpha + \mu)$. Since $a < 0$ and $c > 0$, there is exactly one positive solution I^*.

3.3. Metapopulation model without importation

Disease Free equilibrium and reproductive number. In the absence of importation and with a constant vaccination rate $\alpha_k(t) = \alpha_k^*$ the disease free equilibrium of the metapopulation model is given by

$$S_k^* = \frac{\mu}{\nu\alpha_k^*} N_{0,k}, E_k^* = I_k^* = 0 \text{ and } V_k^* = \frac{\nu\alpha_k^*}{\nu\alpha_* + \mu} N_{0,k}. \tag{10}$$

The basic reproductive ratio, excluding interventions ($\alpha^* = 0$), is given by the largest eigenvalue of the next generation matrix K. We find that

$$K = \frac{\sigma}{(\sigma + \mu)(\delta + \mu)} \begin{bmatrix} \beta_1 N_{0,1} & & 0 \\ & \ddots & \\ 0 & & \beta_n N_{0,n} \end{bmatrix} M.$$

In the absence of movement, where each patch is isolated and therefore $M = I$, the identity matrix, the basic reproductive ratio is given by

$$R_0 = \max_k R_0^k,$$

where $R_0^k = \frac{\sigma\beta_k N_{0,k}}{(\sigma+\mu)(\delta+\mu)}$ is the basic reproductive ratio of patch k.

In the case of homogeneous mixing, where the movement from each patch to any other patch equals one divided by the number of patches and therefore $M = \frac{1}{n}\mathbf{1}$, where $\mathbf{1}$ is a matrix where each entry equals 1, the basic reproductive ratio is given by

$$R_0 = \frac{1}{n}\sum_{k=1}^{n} R_0^k.$$

Theorem 3. *For any migration matrix M satisfying the conditions (C I), (C II) and (C III)*

$$\frac{1}{n\sqrt{n}}\sum_{k=1}^{n} R_0^k \leq R_0 \leq \max_k R_0^k.$$

Table 3
Data used to calibrate the models. For the metapopulation model the number of dogs, number of dog rabies cases and number of vaccinated dogs per week are used for each district. For the homogeneous model the respective values are aggregated over the districts.

District	Number of dogs, $N_{0,k}$	Number of vaccinated dogs	Time of vaccination (Week,Year)
1	1933	925 / 1325 / 62	(42,2012) / (46,2013) / (47,1013)
2	217	64 / 123	(43,2012) / (44,2013)
3	811	376 / 468	(44,2012) / (42,2013)
4	175	24 / 67	(45,2012) / (45,2012)
5	579	311 / 330	(52,2012) / (43,2013)
6	1535	919 / 1044	(46,2012) / (41,2013)
		3342 / 6683 / 503	(47,2012) / (48,2012) / (49,2012)
7	17,273		
		5507 / 4372 / 2699	(48,2013) / (49,2013) / (50,2013)
8	1399	413 / 741	(52,2012) / (51,2013)
9	5672	1929 / 1929 / 4402	(50,2012) / (51,2012) / (51,2013)
10	482	120 / 200	(52,2012) / (51,2013)

Proof. For any nonnegative $n \times n$ matrix A consider the unique matrix G with

$$G \star G = A \star A^T,$$

where $\star$ denotes the element-wise product of two matrices. G is called geometric symmetrization of A. It has been shown ((Schwenk, 1986)) that

$$\rho(A) \geq \rho(G).$$

Since all the entries of K are real and nonnegative, the geometric symmetrization of K is given by $G = (g_{ij})$ with

$$g_{ij} = \sqrt{R_0^i R_0^j m_{ij} m_{ji}}.$$

Since G is symmetric,

$$\rho(G) = ||G||_2,$$

where $||\,||_2$ is the spectral norm. The spectral norm is compatible with the Euclidean norm, which yields

$$||G||_2 \geq \frac{1}{||x||_2} ||Gx||_2,$$

for all $x \in \mathbb{R}^n$ with $||x|| \neq 0$. With $x_j := 1/m_{jj}$ and $||Gx||_2 \geq ||Gx||_\infty$, this yields

$$\begin{aligned}\frac{1}{||x||_2}||Gx||_2 &\geq \frac{1}{||x||_2} \max_k \left(\sum_{j=1}^n \sqrt{R_k R_j m_{kj} m_{jk}} \frac{1}{m_{jj}} \right) \\ &\geq \frac{1}{||x||_2} \sum_{j=1}^n \max_k \left(\sqrt{R_k R_j m_{kj} m_{jk}} \frac{1}{m_{jj}} \right) \\ &\geq \frac{1}{||x||_2} \sum_{j=1}^n R_j.\end{aligned}$$

Since $1/m_{jj} \leq n$ we get

$$\frac{1}{||x||_2} \geq \frac{1}{n\sqrt{n}},$$

which yields

$$\rho(K) \geq \rho(G) \geq \frac{1}{n\sqrt{n}} \sum_{j=1}^n R_j.$$

For the upper bound we use that

$$R_0 = \rho(K) \leq ||K||,$$

for any norm $||\,||$. The basic reproductive number, R_0, is therefore bounded from above by

$$\begin{aligned}||K|| &= \max_{||x||_\infty = 1} ||Ax||_\infty \\ &= \max_k \left\{ \frac{\sigma \beta_k C_k}{(b+\delta)(b+\sigma)} \sum_{j=1}^N |m_{kj}| \right\} \\ &= \max_k R_0^k\end{aligned}$$

□

3.4. Metapopulation model with importation

The metapopulation model with importation has no disease free equilibrium point. We cannot explicitly calculate the endemic equilibrium point, although we expect that there is a unique endemic equilibrium point which is locally asymptotically stable when $R_0 > 1$. We use the mean of the weekly number of cases from the incidence data collected in the 14 weeks before the vaccination campaigns (Table 4) to estimate the pre-intervention weekly incidence of cases ϕ_k^*. We use ϕ_k^* to estimate the endemic equilibrium in each district given by

$$I^* = \frac{1}{\delta}\phi_k^*, \tag{11a}$$

$$E^* = \frac{\delta + \mu}{\sigma} I_k^*, \tag{11b}$$

$$S^* = \frac{\mu N_{0,k}}{\mu + \beta_k \sum_{j=1}^m m_{kj} I_j^*}, \tag{11c}$$

$$V^* = 0. \tag{11d}$$

4. Model calibration

We calibrate the homogeneous and metapopulation model to data on the dog population of N'Djamena, using four years of weekly incidence data, numbers of vaccinated dogs for each district and demographic information. The incidence data (Table 4) comes from passive surveillance of the rabies diagnostic laboratory in N'Djamena. Each case is confirmed with an immunofluorescence antibody test (IFAT) and entered into a database together with basic information on the owner, the status of the animal and the number of bite victims. The data on the total number of dogs and the number of vaccinated dogs was collected during the vaccination campaigns as explained in more detail in a previous publication (Léchenne et al., 2016) and is summarized in Table 3. A recent study (Mindekem et al., 2017) collected data on the number of puppies per litter, the proportion of female dogs with puppies and the age structure of the dogs in N'Djamena. The dog population dynamics in N'Djamena are distinguished by a low average lifespan

Table 4
Weekly number of dog rabies cases and subsequent human exposures over time.

2012														
week	26	27	28	30	32	33	35	36	38	39	40	44	47	50
dog rabies cases	1	1	1	1	1	1	1	1	2	2	1	1	1	1
human exposures	1	2	1	1	2	1	2	1	3	2	6	1	3	7
2013														
week	3	7	23	47										
dog rabies cases	1	1	1	1										
human exposures	3	3	2	4										
2014														
week	6	42												
dog rabies cases	1	1												
human exposures	3	1												
2015														
week	6	8	10	17	21	38								
dog rabies cases	1	1	1	2	1	1								
human exposures	1	1	1	9	1	1								
2016														
week	8	15	16	17	19	20	23	24	28	29	30			
dog rabies cases	1	1	1	1	2	2	1	2	3	2	3			
human exposures	1	2	1	2	2	4	3	3	8	6	9			

(approximately 3 years) and a high mortality of dogs of less than 3 months of age. A common method for estimating birth rates is counting the number of puppies per litter. Death rates are commonly deduced from the average lifespan of dogs. In a population with a high mortality in young age classes, a birth rate estimated from the number of puppies per litter is higher than the death rate estimated from the average lifespan of dogs, which would suggest an exponential increase of the dog population. However, since the dog population is only partially shaped by natural resource availability but mainly by human demand and the number of dogs has remained stable between 2001 (Mindekem et al., 2017) and 2011 (Léchenne et al., 2016), it is reasonable to assume a more or less constant dog population size. When calibrating a model to demographic data, this can be achieved by introducing a carrying capacity, which yields an additional death rate and a subsequent increased population turnover. However, since young dogs are often not vaccinated this leads to an over estimation of the overall immunity loss of the population after a vaccination campaign. We therefore use a constant birth and death rate μ, deduced from the average lifespan of 3 years.

For the metapopulation model, we divide the city into 10 patches, where the patches correspond to the districts that are shown in Fig. 1, since the incidence data we use is aggregated at district level. The stable population size in each district, $N_{0,\,k}$, is estimated in a recent publication (Léchenne et al., 2016) and summarised in Table 3. We estimate the entries of the migration matrix M assuming equal movement between any two adjacent patches, no direct movement between patches that share no border and, based on the results in Smith et al. (2001), a 7-fold reduction of movement across the river. This yields the following migration matrix:

$$M = \begin{bmatrix} m_{1,1} & p & 0 & 0 & 0 & 0 & 0 & 0 & 0 & p \\ p & m_{2,2} & p & p & 0 & 0 & 0 & p & 0 & p \\ 0 & p & m_{3,3} & p & p & p & 0 & 0 & rp & 0 \\ 0 & p & p & m_{4,4} & p & 0 & 0 & p & 0 & 0 \\ 0 & 0 & p & p & m_{5,5} & p & p & p & 0 & 0 \\ 0 & 0 & p & 0 & p & m_{6,6} & p & 0 & rp & 0 \\ 0 & 0 & 0 & 0 & p & p & m_{7,7} & p & rp & 0 \\ 0 & p & 0 & p & p & 0 & p & m_{8,8} & 0 & p \\ 0 & 0 & rp & 0 & 0 & rp & rp & 0 & m_{9,9} & 0 \\ p & p & 0 & 0 & 0 & 0 & 0 & p & 0 & m_{10,10} \end{bmatrix}$$

with $r = 1/7$, $m_{ii} = 1 - \sum_{j \neq i} m_{ij}$ and p bounded above so that conditions (C I), (C II) and (C III) are satisfied. We fit a separate transmission rate, β_k, and importation rate, ε_k, for each district and the proportion of dogs moving, p, to the four years of weekly incidence data from N'Djamena, by minimising the squared Euclidean distance between the simulated weekly incidence and the data. For the initial fitting we assume no underreporting. Other rabies biology parameters, such as the incubation period, $1/\sigma$, are taken from literature. The data on number of dogs, dog rabies cases and vaccinated dogs for each district is displayed in Table 3. The baseline parameter values are summarised in Table 5. The fitted parameter values for each district are shown in Table 6. cases:

We fit the vaccination rates, $\alpha_k(t)$, to the data from the vaccination campaigns as described in more detail in a previous publication (Zinsstag et al., 2017). In each patch the vaccination rate, $\alpha_k(t)$, is given by

$$\alpha_k(t) = \alpha_k^* + \alpha_{0,k}^{(i)}(t) + \alpha_{1,k}^{(i)}(t) e^{-\varphi_\alpha t}, \tag{12}$$

where α_k^* is a constant background vaccination rate, $\alpha_{0,k}^{(i)}$ and $\alpha_{1,k}^{(i)}$ are fit to the number of vaccinated dogs in patch k in week i and φ_α is a constant auxiliary parameter, that we set to $\varphi_\alpha = 100$. The auxilliary parameter φ_α is the slope of the change of the vaccination rate from one week to the next. By using a high absolute value of φ_α we assure that the function $\alpha_k(t)$ changes its value at the beginning of each new week of the vaccination campaigns while assuring that the function $\alpha_k(t)$ is differentiable. We assume that in each patch k and each week i the number of unvaccinated dogs, U, and vaccinated dogs, V, satisfy the following equations

$$\frac{dU}{dt} = \mu N_{0,k} - \alpha_k^{(i)} - \mu U, \tag{13a}$$

$$\frac{dV}{dt} = \alpha_k^{(i)} U, \tag{13b}$$

with $\alpha_k^{(i)} = \alpha_{0,k}^{(i)} + \alpha_{1,k}^{(i)} e^{-\varphi_\alpha t}$. The Eqs. (13) correspond to the model described in Eqs. (3), in the absence of rabies transmission ($\beta = 0$) and ignoring the death of vaccinated dogs ($\mu V = 0$). The total number of dogs in each patch, $N_{0,\,k}$, and the number of vaccinated dogs in each patch and each week of the vaccination campaigns are given in Table 3. For the weeks during the vaccination campaigns we fit $\alpha_{0,k}^{(i)}$ and $\alpha_{1,k}^{(i)}$ by minimising the squared Euclidean distance between the simulated number of vaccinated dogs and the data on the number of vaccinated dogs collected during the campaigns that are summarised in Table 3. For all other weeks $\alpha_k^{(i)} = 0$. For the homogeneous model the same procedure can be applied by fitting $\alpha_0^i(t)$ and $\alpha_1^i(t)$ to the sum of the number of vaccinated dogs over all the patches.

Table 5
Parameter values of the rabies transmission model. Time is measured in weeks.

	Description	Value	Unit	Range	Source
μ	Birth rate	0.0066	1/time	[0.0013, 0.0192]	field study, Mindekem et al. (2017)
σ	Inverse incubation period	0.239	1/time	[0.01, 1]	previous model, Zinsstag et al. (2009)
δ	Disease induced death rate	1.23	1/time	[1, 7]	previous model, Zinsstag et al. (2009)
ν	Efficacy of vaccine	0.95	dimensionless	[0.8, 1]	previous model, Zinsstag et al. (2009)

Table 6
Values for the fitted transmission rates, β_k, importation rates, ε_k, and movement proportions, p, for the different models. Values displayed over a whole column apply to all districts.

	Metapopulation model, importation			Metapopulation model, no importation		Homogeneous model, importation		Homogeneous model, no importation
k	$\beta_k(10^{-4})$	$\varepsilon_k(10^{-2})$	$p(10^{-4})$	$\beta_k(10^{-4})$	$p(10^{-2})$	$\beta(10^{-5})$	$\varepsilon(10^{-1})$	$\beta(10^{-5})$
1	4.855	7.21	2.21	4.73	4.05	3.45	1.362	4.26
2	0.029	0		1.88				
3	0.745	0		2.48				
4	3.040	0		3.02				
5	20.87	0.36		0				
6	0.140	0		60.03				
7	0.713	4.03		0.702				
8	0.437	0		0.01				
9	1.400	6.26		2.39				
10	6.631	0		2.65				

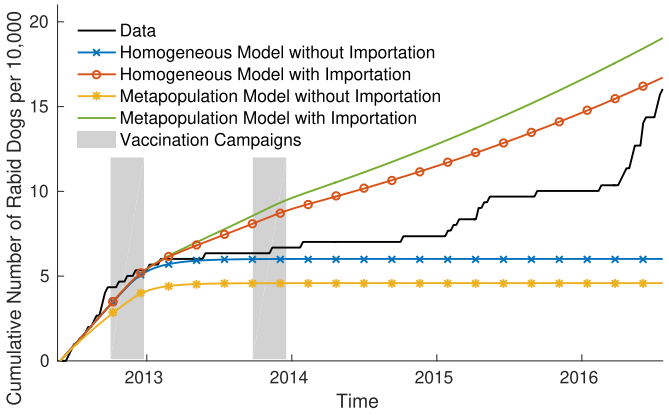

Fig. 3. Incidence data from N'Djamena (black line) and cumulative number of rabid dogs in the four different models.

5. Numerical simulations and sensitivity analysis

5.1. Simulation results of the deterministic models

We numerically solve the model Eqs. (1) and (3) using MATLAB (with the Runge–Kutta solver `ode45`). We use the pre-intervention endemic equilibrium calculated from the incidence data before the vaccination campaigns as an initial condition and fit the transmission rates, β_k, the movement parameter, p, and the importation rates, ε_k, by minimising the squared Euclidean distance between the simulated weekly incidence and the data. The simulated cumulative incidence by the best fitting parametrization are shown in Fig. 3. Both models without importation show an interruption of transmission after the first vaccination campaign. We therefore conclude that in our model framework, heterogeneity alone does not explain the resurgence of cases. The models with importation perform similarly well and capture the resurgence of cases after the campaigns that is seen in the data.

5.2. Stochastic implementation of the models

Deterministic models are useful to provide analytical results and to derive equilibria and threshold conditions. However, they do not capture random events which can be important in a system with low numbers of cases. We therefore implement a stochastic version of our model which allows us to capture random events an to explore the distribution of the time to elimination.

Simulations of elimination without importation. In the absence of importation, the weekly incidence declines after the first vaccination campaign. We used the stochastic implementation of the homogeneous and the metapopulation model without importation to explore the distribution of the time to elimination. The stochastic simulations in Fig. 4 show that it is likely that rabies could die out even without vaccination, because of the low number of cases. This further suggests that importation is necessary for persistence of rabies transmission. Comparing the time to elimination with vaccination in the homogeneous and the metapopulation model shows that accounting for heterogeneity in dog densities and vaccination coverages did not alter the time to elimination. This suggests that even though vaccination coverage varied across the different districts of the city, there was no district with a coverage low enough to permit pockets of ongoing transmission, which would have been captured by the metapopulation model.

Simulations of cases averted with importation. In the model with importation, there can be interruption of transmission but no permanent elimination. We used the stochastic version of the homogeneous model with importation to estimate the average number of dog rabies cases per year in the case of no vaccination. We incorporated parameter uncertainty using a Bayesian sampling resampling approach. We created an initial sample of 10,000 parameter sets in a subset of $\mathbb{R}^5$, using Latin hypercube sampling with values for μ, σ, δ and ν drawn from uniform distributions with ranges shown in Table 5 and ε uniformly drawn from the range [0,0.1]. For each set of parameter values, we computed the likelihood of the simulation results of the model with the vaccination campaigns to the data using a Poisson likelihood given by

$$\mathcal{L}(\theta|x) = \prod_{i=1}^{n} \frac{\theta_i^{x_i}}{x_i!} e^{-\theta_i}, \tag{14}$$

where x_i is the incidence data in week i and θ_i is the simulated incidence in week i. We resampled 1000 sets of parameter values (with replacement) based on their likelihood from the initial

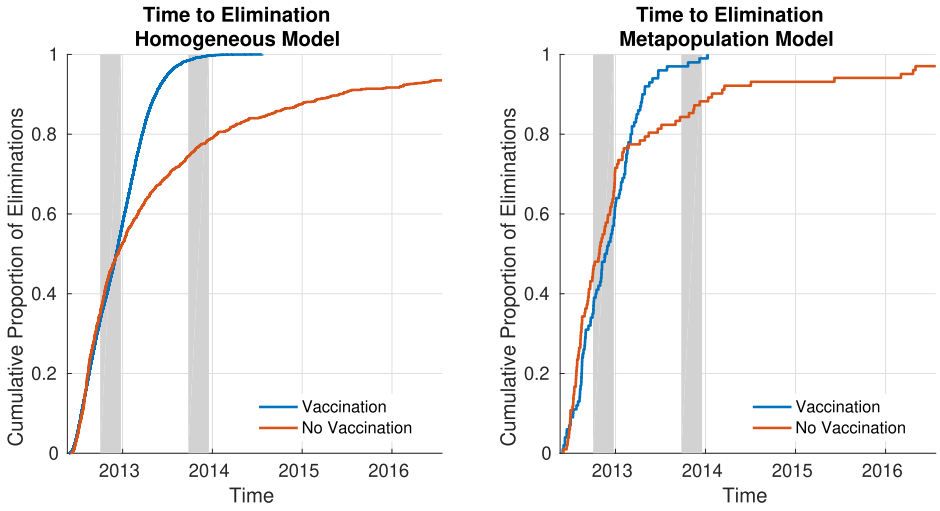

Fig. 4. Time to elimination in the stochastic implementation of the homogeneous and the metapopulation model in the absence of importation with vaccination (blue line) and without vaccination (red line). (For interpretation of the references to colour in this figure legend, the reader is referred to the web version of this article.)

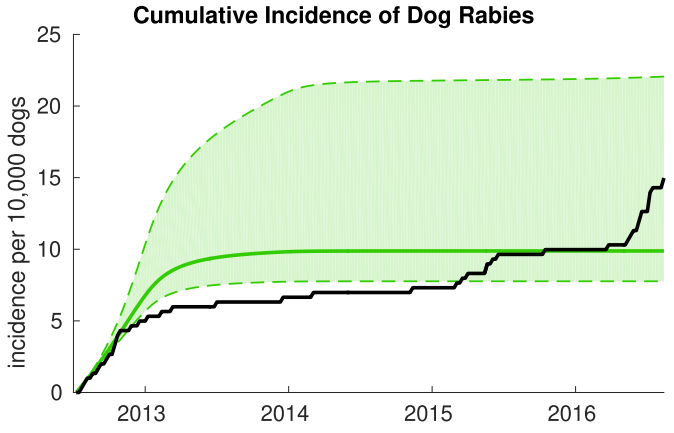

Fig. 5. Sensitivity analysis of the cumulative number of cases with respect to detection probability. The black line is the reported number of cases. The green line and interval represents the median and the 95% credible interval of the estimated number of cases for different reporting probabilities.

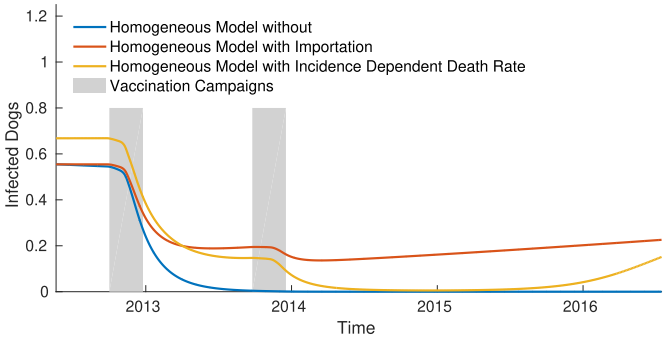

Fig. 6. Infective dogs over time for homogeneous models without importation (blue line, $\beta = 4.26 \cdot 10^{-5}, \varepsilon = 0$), with importation (red line, $\beta = 3.45 \cdot 10^{-5}, \varepsilon = 0.1362$) and without importation but with an incidence dependent disease induced death rate (yellow line, $\beta = 1.0 \cdot 10^{-4}, \varepsilon = 0$). (For interpretation of the references to colour in this figure legend, the reader is referred to the web version of this article.)

10,000 samples. We simulated the stochastic model for these 1000 parameter sets assuming no vaccination campaigns. We found that in the absence of vaccination campaigns, the average number of cases per year was 37, with an interquartile range of (34,42). In the years 2013 and 2014, after the first and the second vaccination campaign, there were 7 cases of dog rabies in N'Djamena. This implies that over two years, 67 cases of rabies were averted by the vaccination campaigns.

The surveillance data also includes the number of human exposures for each rabid dog (Table 4). We use the MATLAB function `poissfit` to fit a Poisson distribution to the number of humans bitten by each rabid dog, yielding an estimated mean of 2.0159 human exposures per dog. We translated the number of dog rabies cases averted, for each simulation run, to the number of human exposures averted by sampling a number of human exposures for each dog rabies case from this distribution. We estimate that the vaccination campaigns averted approximately 124 (82, 214) human exposures over two years.

5.3. Underreporting

To assess the impact of underreporting on the transmission dynamics, we assumed that each true rabies case is reported to the rabies diagnostic laboratory with a detection probability p. The rabies diagnostic laboratory conducting the immunofluorescence antibody test (IFAT) is situated in district 1 in the west of N'Djamena, whereas most cases are reported from districts 7 and 9 at the north-east of the city. We therefore assume that reporting cases is not dependent on the distance to the laboratory and assume a homogeneous rate of underreporting across all districts. We ran 10,000 simulations of the homogeneous model sampling the detection probability p from a uniform distribution in the range [0.01, 1] and used it to estimate the true number of cases from the reported cases, which we then used for fitting the transmission rate, β. While the absolute number of cases depends on the detection probability, p, the overall dynamics of the cumulative incidence curve are not affected by the underreporting as shown in Fig. 5.

5.4. Simulations with an incidence dependent disease induced death rate

An alternative explanation for the early resurgence could be that the cases in the data are produced by a series of small epidemics that are repeatedly ended by a raised alertness in the population and a subsequent increased death rate of rabid dogs. To investigate the impact of this assumption we conduct a theoretical

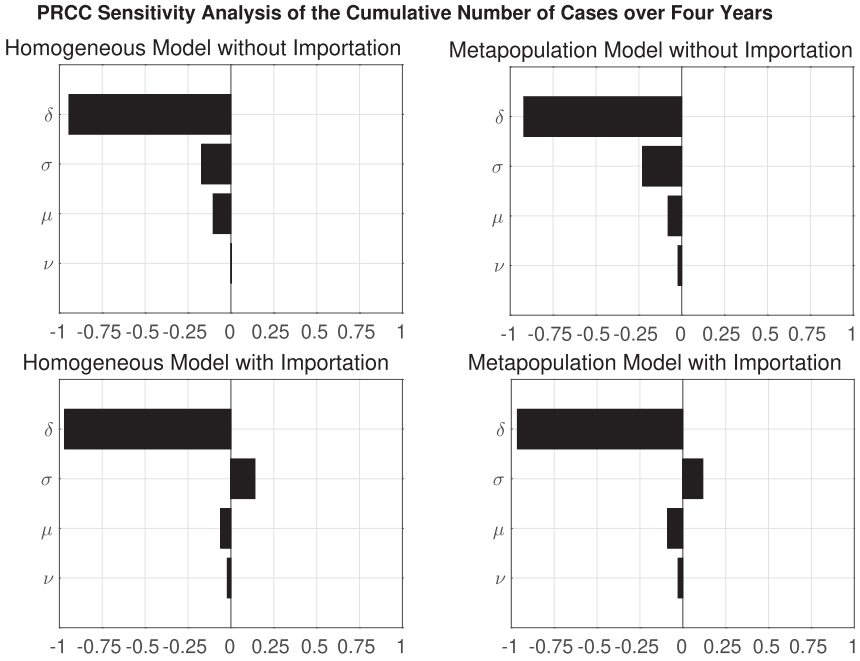

Fig. 7. Partial rank correlation coefficient analysis of the cumulative number of cases over four years for the four different models.

exercise with the following equations:

$$\frac{dS(t)}{dt} = \mu N_0 - (\nu\alpha(t) + \mu)S(t) - \beta S(t)I(t), \tag{15a}$$

$$\frac{dE(t)}{dt} = \beta S(t)I(t) - (\sigma + \mu)E(t), \tag{15b}$$

$$\frac{dI(t)}{dt} = \sigma E(t) - (\delta(I(t)) + \mu)I(t), \tag{15c}$$

$$\frac{dV(t)}{dt} = \nu\alpha(t)S(t) - \mu V(t). \tag{15d}$$

where

$$\delta(I(t)) = \delta_0 + (\delta_1 - \delta_0)(1 - e^{-\varphi_\delta I(t)}).$$

The parameters δ_0 and δ_1 correspond to the upper and lower bound of the disease induced death rate. We assume that if rabies is not present in the population the disease induced death rate is equal to the baseline value ($\delta_0 = 1.23$). As rabies incidence increases the disease induce death rate, $\delta(I(t))$, approaches a hypothetical value of $\delta_1 = 7$, which corresponds to a scenario where each infected dog is killed on average one day after it first shows symptoms. We choose a hypothetical value for the saturation parameter ($\varphi_\delta = 0.5$) and a high transmission rate ($\beta = 1.0 \cdot 10^{-4}$). Although we cannot analytically compute the endemic equilibrium point for this system, we can numerically simulate the time evolution of the system. The incidence over time of the homogeneous model with and without importation, and with the incidence dependent death rate are shown in Fig. 6. The model with the incidence dependent death rate also shows the observed resurgence in cases after the vaccination campaigns. The hypothesis that transmission is in fact higher than estimated from the incidence data and that rabies is kept under control by small scale local interventions could therefore also be a potential explanation of the pattern we see in the data.

5.5. Sensitivity analysis

We conducted global sensitivity analysis of the cumulative number of cases over four years to four model parameters (δ, σ, μ and ν) for the homogeneous and metapopulation models, with and without importation. We ran 10,000 simulations, drawing values for the parameters with ranges given in Table 5 assuming uniform distributions, and fit the transmission rates β_k for each simulation run. We calculated the partial rank correlation coefficients (PRCC) of the cumulative incidence over four years to the model parameters. The results in Fig. 7 show that all models are very sensitive to the disease induced death rate, δ. This is because the disease induced death rate determines for how long a dog is infectious and therefore has a crucial impact on the transmission dynamics. If the transmission rate, β_k, were constant, the sensitivity to the incubation period, $1/\sigma$, would be positive in all models, because as σ increases, the duration of the incubation period decreases, and the probability that a dog survives the exposed period increases, leading to a higher number of cases. However, because we fit the transmission rates, β_k, for each set of parameter values, the best fitting β_k for models without importation were lower for higher values of σ, leading to a lower number of cases. In the models with importation, the introduction of exposed dogs compensates for this and leads to a higher number of cases. The mortality and birth rate, μ, mainly influences the transmission dynamics via the loss of vaccination coverage in the population after a campaign due to the death of vaccinated dogs and the birth of unvaccinated dogs. However the cumulative number of cases is not very sensitive to this population turnover of dogs.

6. Discussion and conclusion

After two mass vaccination campaigns of dogs in N'Djamena in 2012 and 2013, rabies transmission was interrupted for several months. However, there was a resurgence in dog rabies cases, which was not predicted by previous models of rabies transmission. We used deterministic compartmental models to explore different reasons for this early resurgence. These hypotheses include

heterogeneity, importation of exposed dogs and underreporting of rabies cases with higher levels of ongoing transmission in certain districts. Dog densities and vaccination coverage varied substantially across the districts of N'Djamena (Fig. 1) because of differences in attitudes towards dog ownership depending on the sociocultural backgrounds (Léchenne et al., 2016). Our results suggest that heterogeneity alone does not explain the resurgence in cases, whereas importation of cases is a plausible explanation of the incidence data. Our analysis of underreporting suggests that while it alters the number of cases, it does not affect the transmission dynamics, so it is an unlikely explanation of the resurgence. Simulations of the stochastic versions of our models estimated that the vaccination campaigns averted approximately 67 cases of dog rabies over two years.

Since our models suggest importation of cases was the likely cause of resurgence within the city, preventing the introduction of latent dogs, possibly by monitoring the vaccination status of incoming dogs, would help to maintain a longer duration without rabies. Alternatively, longer lasting vaccination coverage could be achieved by repeated mass vaccination campaigns or continuous vaccination through the veterinary health system to lengthen the period of herd immunity. Since the dog population turnover substantially influences the overall immunity loss of the population, increasing the lifespan of vaccinated dogs would also be beneficial. Furthermore, interventions that target rabid dogs and quickly remove them from the system could suppress transmission. An efficient surveillance system could therefore substantially contribute to rabies control.

Our models assumed density dependent transmission of rabies and a homogeneous dog population within each patch of the metapopulation model. Even though this approach captures the heterogeneity in dog densities and vaccination coverage at district level, it does not account for the fine scale contact structure among the dogs in each district. Future work is needed to show how this contact structure among the dogs could influence the transmission dynamics of rabies.

Our analyses estimated that the dog vaccination campaigns averted about 124 human exposures over two years. Dog vaccination is therefore an effective tool to reduce human cases and can contribute to the goal of zero rabies deaths by 2030.

Acknowledgements

This work was supported by the Swiss National Science Foundation under grant number 310030 160067. The authors thank Peter Pemberton-Ross, Timo Smieszek and Thomas Smith for helpful comments and discussions.

References

Anderson, R.M., Jackson, H.C., May, R.M., Smith, A.M., 1981. Population dynamics of fox rabies in Europe. Nature 289 (2), 765–770.

Beyer, H.L., Hampson, K., Lembo, T., Cleaveland, S., Kaare, M., Haydon, D.T., 2011. Metapopulation dynamics of rabies and the efficacy of vaccination. Proc. R. Soc. Lond. B 278 (1715), 2182–2190. doi:10.1098/rspb.2010.2312.

Bourhy, H., Nakouné, E., Hall, M., Nouvellet, P., Lepelletier, A., Talbi, C., Watier, L., Holmes, E.C., Cauchemez, S., Lemey, P., Donnelly, C.A., Rambaut, A., 2016. Revealing the micro-scale signature of endemic zoonotic disease transmission in an African urban setting. PLoS Pathog. 12 (4), 1–15. doi:10.1371/journal.ppat.1005525.

Castillo-Neyra, R., Brown, J., Borrini, K., Arevalo, C., Levy, M.Z., Buttenheim, A., Hunter, G.C., Becerra, V., Behrman, J., Paz-Soldan, V.A., 2017. Barriers to dog rabies vaccination during an urban rabies outbreak: qualitative findings from Arequipa, Peru. PLoS Negl. Trop. Dis. 11 (3), 1–21. doi:10.1371/journal.pntd.0005460.

Chen, J., Zou, L., Jin, Z., Ruan, S. , 2015. Modeling the geographic spread of rabies in China. PLoS Negl. Trop. Dis. 9 (5), 1–18. doi:10.1371/journal.pntd.0003772.

Diekmann, O., Heesterbeek, J.A.P., Roberts, M.G., 2010. The construction of next-generation matrices for compartmental epidemic models. J. R. Soc. Interface doi:10.1098/rsif.2009.0386.

Dürr, S., Ward, M.P., 2014. Roaming behaviour and home range estimation of domestic dogs in aboriginal and torres strait islander communities in northern australia using four different methods. Prev. Vet. Med. 117 (2), 340–357.

Dürr, S., Ward, M.P., 2015. Development of a novel rabies simulation model for application in a non-endemic environment. PLoS Negl. Trop. Dis. 9 (6), 1–22. doi:10.1371/journal.pntd.0003876.

Fahrion, A.S., Taylor, L.H., Torres, G., Muller, T., Durr, S., Knopf, L., de Balogh, K., Nel, L.H., Gordoncillo, M.J., Abela-Ridder, B., 2017. The road to dog rabies control and elimination-what keeps us from moving faster? Front Public Health 5, 103.

Fooks, A.R., Banyard, A.C., Horton, D.L., Johnson, N., McElhinney, L.M., Jackson, A.C., 2014. Current status of rabies and prospects for elimination. Lancet 384 (9951), 1389–1399. doi:10.1016/S0140-6736(13)62707-5.

Gillespie, D.T., 1977. Exact stochastic simulation of coupled chemical reactions. J. Phys. Chem. 81 (25), 2340–2361.

Hampson, K., Coudeville, L., Lembo, T., Sambo, M., Kieffer, A., Attlan, M., Barrat, J., Blanton, J.D., Briggs, D.J., Cleaveland, S., Costa, P., Freuling, C.M., Hiby, E., Knopf, L., Leanes, F., Meslin, F.-X., Metlin, A., Miranda, M.E., Müller, T., Nel, L.H., Recuenco, S., Rupprecht, C.E., Schumacher, C., Taylor, L., Vigilato, M.A.N., Zinsstag, J., Dushoff, J., on behalf of the Global Alliance for Rabies Control Partners for Rabies Prevention, 2015. Estimating the global burden of endemic canine rabies. PLoS Negl. Trop. Dis. 9 (4), 1–20. doi:10.1371/journal.pntd.0003709.

Hampson, K., Dushoff, J., Cleaveland, S., Haydon, D.T., Kaare, M., Packer, C., Dobson, A., 2009. Transmission dynamics and prospects for the elimination of canine rabies. PLoS Biol. 7 (3), 1–10. doi:10.1371/journal.pbio.1000053.

Keller, J.P., Gerardo-Giorda, L., Veneziani, A., 2013. Numerical simulation of a susceptible-exposed-infectious space-continuous model for the spread of rabies in raccoons across a realistic landscape. J. Biol. Dyn. 7 (sup1), 31–46. PMID: 23157180, doi: 10.1080/17513758.2012.742578.

Kessels, J.A., Recuenco, S., Navarro-Vela, A.M., Deray, R., Vigilato, M., Ertl, H., Durrheim, D., Rees, H., Nel, L.H., Abela-Ridder, B., Briggs, D., 2017. Pre-exposure rabies prophylaxis: a systematic review. Bull. World Health Organ. 95 (3), 210–219.

Lakshmanan, N., Gore, T.C., Duncan, K.L., Coyne, M.J., Lum, M.A., Sterner, F.J., 2006. Three-year rabies duration of immunity in dogs following vaccination with a core combination vaccine against canine distemper virus, canine adenovirus type-1, canine parvovirus, and rabies virus. Vet. Ther. 7 (3), 223–231.

Lankester, F., Hampson, K., Lembo, T., Palmer, G., Taylor, L., Cleaveland, S., 2014. Implementing pasteur's vision for rabies elimination. Science 345 (6204), 1562–1564. doi:10.1126/science.1256306.

Lembo, T., Hampson, K., Kaare, M.T., Ernest, E., Knobel, D., Kazwala, R.R., Haydon, D.T., Cleaveland, S., 2010. The feasibility of canine rabies elimination in africa: dispelling doubts with data. PLoS Negl. Trop. Dis. 4 (2), 1–9. doi:10.1371/journal.pntd.0000626.

Mindekem, R., Léchenne, M., Alfaroukh, I.O., Moto, D.M., Zinsstag, J., Ouedraogo, L.T., Salifou, S., 2017. Dynamique de la population canine et risque de transmission du virus de la rage dans les districts sanitaires de Laoukassy, Bénoze, Moundou et N'Djaména sud au Tchad. Rev. Cames Sante 5 (1).

Léchenne, M., Oussiguere, A., Naissengar, K., Mindekem, R., Mosimann, L., Rives, G., Hattendorf, J., Moto, D.D., Alfaroukh, I.O., Zinsstag, J., 2016. Operational performance and analysis of two rabies vaccination campaigns in N'djamena, chad. Vaccine 34 (4), 571–577. doi:10.1016/j.vaccine.2015.11.033.

Murray, J.D., Stanley, E., Brown, D., 1986. On the spatial spread of rabies among foxes. Proc. R. Soc. Lond. 229 (2), 111–150.

Ou, C., Wu, J., 2006. Spatial spread of rabies revisited: influence of age-dependent diffusion on nonlinear dynamics. SIAM J. Appl. Math. 67 (1), 138–163. doi:10.1137/060651318.

World Health Organization, 2010. Rabies vaccines: WHO position paper - recommendations. Vaccine 28 (44), 7140–7142. doi: 10.1016/j.vaccine.2010.08.082.

Schwenk, A.J., 1986. Tight bounds on the spectral radius of asymmetric nonnegative matrices. Linear Algebra Appl. 75 (1).

Smith, D.L., Lucey, B., Waller, L.A., Childs, J.E., Real, L.A., 2001. Predicting the spatial dynamics of rabies epidemics on heterogeneous landscapes. Proc. Natl. Acad. Sci. U.S.A. 99 (6).

World Health Organization, 2013. WHO Expert Consultation on Rabies: Second Report. Technical Report. World Health Organization.

Zinsstag, J., Dürr, S., Penny, M.A., Mindekem, R., Roth, F., Gonzalez, S.M., Naissengar, S., Hattendorf, J., 2009. Transmission dynamics and economics of rabies control in dogs and humans in an african city. Proc. Natl. Acad. Sci. 106 (35), 14996–15001. doi:10.1073/pnas.0904740106.

Zinsstag, J., Lechenne, M., Laager, M., Mindekem, R., Naïssengar, S., Oussiguéré, A., Bidjeh, K., Rives, G., Tessier, J., Madjaninan, S., Ouagal, M., Moto, D.D., Alfaroukh, I.O., Muthiani, Y., Traoré, A., Hattendorf, J., Lepelletier, A., Kergoat, L., Bourhy, H., Dacheux, L., Stadler, T., Chitnis, N., 2017. Vaccination of dogs in an african city interrupts rabies transmission and reduces human exposure. Sci. Transl. Med. 9 (421). doi:10.1126/scitranslmed.aaf6984.